Analytical and Bioanalytical Chemistry (2019) 411:559–564
https://doi.org/10.1007/s00216-018-1300-7

COMMUNICATION

Gold nanoparticles as labels for immunochemical analysis using laser ablation inductively coupled plasma mass spectrometry

Michaela Tvrdonova[1,2] · Marcela Vlcnovska[3] · Lucie Pompeiano Vanickova[3,4] · Viktor Kanicky[1,2] · Vojtech Adam[3,4] · Lena Ascher[5] · Norbert Jakubowski[5] · Marketa Vaculovicova[3,4] · Tomas Vaculovic[1,4]

Received: 5 June 2018 / Revised: 20 July 2018 / Accepted: 27 July 2018 / Published online: 14 August 2018

Abstract

In this paper, we describe the labelling of antibodies by gold nanoparticles (AuNPs) with diameters of 10 and 60 nm with detection by laser ablation inductively coupled plasma mass spectrometry (LA-ICP-MS). Additionally, the AuNPs labelling strategy is compared with commercially available labelling reagents based on MeCAT (metal coded affinity tagging). Proof of principle experiments based on dot blot experiments were performed. The two labelling methods investigated were compared by sensitivity and limit of detection (LOD). The absolute LODs achieved were in the range of tens of picograms for AuNP labelling compared to a few hundred picograms by the MeCAT labelling.

Keywords Dot blot · Antibody labelling · Gold nanoparticles · LA-ICP-MS · Immunochemistry

Introduction

Since the 1980s, colloidal gold has been used for immunohistochemical staining of proteins in membrane-based immunoassays [1–3]. The intensive purple color enables a colorimetric detection of the labelled molecules concentrated at the surface of the membrane (after electroblotting) so that limits of detection at the level of attomolar concentrations [4] can be achieved. Sometimes, several labels are used simultaneously (e.g., colloidal gold and peroxidase or alkaline phosphatase) for the detection of multiple antigen spots on a single blot membrane [4]. Besides this experimentally simple colorimetric detection, other more instrumentally demanding but more sensitive techniques are also discussed, including fluorescent, electrochemical, or calorimetric detection [5].

Metallic nanoparticles had already been applied for detection of biomolecules inside a single cell by use of surface enhanced Raman spectroscopy (SERS). In the case of gold nanoparticles, the local fields generated upon excitation of their localized surface plasmons enable sensitive probing of the molecules interacting with the particle surface on the nanometer scale within living cells by surface-enhanced Raman scattering (SERS) [6–9]. SERS can also be used for sensing of general chemical parameters in the cellular nano-environment. For example, progressing acidification in endosomes [10, 11] using nanoprobes containing a pH-sensitive reporter molecule [12, 13].

Inductively coupled plasma mass spectrometry (ICP-MS) is a well-established method for multi-elemental analysis of elements at trace and ultra-trace levels. It has found acceptance in various application areas over the last decade. ICP-MS is more suitable for detection in the life sciences. For these applications, ICP-MS excels in a high sensitivity which is independent of the molecular structure of the analyte, a wide linear dynamic range and by excellent multi-element capabilities. In combination with laser ablation as a sample introduction system for the analysis of soft materials it has also been used extensively for bioimaging (for more details, see review

Published in the topical collection *Elemental and Molecular Imaging by LA-ICP-MS* with guest editor Beatriz Fernández García.

✉ Tomas Vaculovic
vaca_777@yahoo.com

[1] Department of Chemistry, Faculty of Science, Masaryk University, Kamenice 753/5, 625 00 Brno, Czech Republic

[2] CEITEC, Masaryk University, Kamenice 753/5, 625 00 Brno, Czech Republic

[3] Department of Chemistry and Biochemistry, Mendel University in Brno, Zemedelska 1, 613 00 Brno, Czech Republic

[4] Central European Institute of Technology, Brno University of Technology, Purkynova 123, 612 00 Brno, Czech Republic

[5] Bundesanstalt für Materialforschung und -prüfung (BAM), Richard-Willstätter-Straße 11, 12489 Berlin, Germany

[14]). Recently, LA-ICP-MS has also been used to image the distribution of metallic nanoparticles (Au, Ag) in single biological cells [15].

The first immunoassay for detection of thyroxine in solution was described by Zhang et al. [16], and the history of immuno-histochemical approaches developed for ICP-MS applications has already been discussed extensively in review articles [17]. The combination of immunoassays and ICP-MS can be carried out through proper elemental tagging [18]. High multiplexing and signal amplification capabilities are the main advantages of using metal chelates, e.g., 1,4,7,10-tetraazacyclododecane-1,4,7,10-tetraacetic acid (also known as DOTA) coordinated with heteroatoms (typically lanthanide ions) for elemental tagging. Significant signal improvements have been achieved by the use of polymeric tags containing metal ions, such as MAXPAR™ for application in Western blot assays [19]. In the case of polymeric tags, signal amplification has been achieved by the coupling of a single polymer chain carrying more than 100 lanthanide elements per Ab compared to the previously mentioned metal chelates. Waentig et al. found that MAXPAR™ gives better sensitivity than DOTA and MeCAT (metal coded affinity tag), respectively. However, due to a higher background signal, the S/N ratio and finally the limits of detection (LOD: fmol range) are worse than that for MeCAT.

Even higher amplification factors have been achieved in a Western blot approach discussed by Mueller et al. [20]. They followed the concept of Western blotting after separation by gel electrophoresis and used gold cluster-labelled antibodies for detection by laser ablation ICP-MS for the determination of the Mre11 protein in crude lysates of CHO-K1 fibroblasts. This protein is essential for mediating genome stability and DNA repair in mammalian cells. In this approach, high sensitivities have been achieved using an antibody conjugated to gold nanoclusters. More than 50,000 gold atoms can be attached to each antibody at once by this technique, which can help to reach limits of detection below 1 fmol of protein. More recently, Cruz-Alonso et al. used a new immuno-histochemical-based procedure to study the distribution of metallothionein ½ (MT ½) and metallothionein 3 (MT 3) in human retina tissue. For this purpose, antibodies (Ab) were bio-conjugated by gold nanoclusters (AuNCs) and labelled in combination with laser ablation (LA) coupled to ICP-MS for detection. Each cluster with a diameter of 2.7 nm contained roughly 580 atoms. [21]

Overall, one can summarize that application of Au nanoparticles and clusters look promising for bio-conjugation to improve the signal intensity in LA-ICP-MS; however, as has been mentioned, other factors such as unspecific binding can lead to a reduced S/N ratio or the labelling process can have an impact on the specificity of the antibody. In this work, we have developed a methodology for the tagging of antibodies via gold nanoparticles to enhance the signal intensity in LA-ICP-MS. Hence, we performed a proof of principle experiment based on dot blot experiments to demonstrate the improvement in sensitivity and specificity of the AuNP conjugation of antibodies in comparison with reagents based on the MeCAT technology as a reference.

Materials and methods

Chemicals

The following chemicals were used: Milli-Q water (purification system, Millipore, Bedford, MA). All solutions were prepared using this ultrapure water. Milk powder, Tris-buffered saline including 0.1% Tween 20, pH 7.3 (TBS-T), Tris buffer (20 mM Tris; 150 mM NaCl; 2.5 mM EDTA (pH 7), metal coded affinity tag MeCAT (Proteome Factory, Berlin, Germany), tris(2-caboxyethyl)phosphine*HCl (TCEP), GOLD Conjugation Kit (60 nm, 20 OD) ab 188,216 and GOLD Conjugation Kit (10 nm, 20 OD) ab201808 Abcam, Goat anti-mouse antibody Abcam (ab6708, Cambridge, UK, 2 mg/ml), Mouse immunoglobulin, Abcam (ab198772, Cambridge, UK).

Nanoparticle-antibody conjugation

Gold nanoparticle (10 and 60 nm) conjugation kits were purchased from Abcam (ab188216, ab201808, Cambridge, UK) and the conjugation was carried out according to the manufacturer's instructions. Briefly, 2 mg/ml of goat anti-mouse antibody was diluted to an appropriate concentration with a buffer provided. This solution was mixed with gold nanoparticles and left to react for 15 min. Finally, a quencher provided in the kit was added and the mixture was left for 5 min to stop the conjugation reaction.

MeCAT antibody labelling

Antibody labelling with metal-coded affinity tag MeCAT (Proteome Factory, Berlin, Germany) containing holmium as the elemental tag was performed in accordance with the publication of Waenting et al. [19]

Dot blot preparation

Mouse immunoglobulin was used as a model antigen and goat anti-mouse antibody was employed as the testing antibody. The dot blot analysis was carried out using a polyvinylidene fluoride (PDVF) membrane (Bio-rad, Prague, Czech Republic). First, the membrane was activated by immersing it in methanol for 30 s and then in blotting buffer containing 50%$_{(v/v)}$ of buffer (25 mM Trizma base, 150 mM glycine, 10% $_{(v/v)}$ methanol), and 10%$_{(v/v)}$ MetOH for 30 s.

0.5 μl of the antigen solution were pipetted onto the membrane which resulted in a dot diameter of approximately 0.8 mm. On each membrane, seven dots with increasing concentration of antigen were applied (0.1, 0.2, 0.5, 1.0, 5.0, and 10 ng/ml). Subsequently, the membrane was blocked for 30 min in blocking buffer (10% milk powder, 90% phosphate buffer saline Sigma Aldrich, USA). The membrane was then incubated in a solution of a marked antibody (6.7 ng/ml) for 1 h at room temperature. Finally, the membrane was washed three times by 0.05% solution of Tween 20 in phosphate buffer saline to remove the non-bound antibodies.

LA-ICP-MS analysis

LA-ICP-MS analysis of the dot blots was undertaken by a laser ablation system UP213 (NewWave, USA) emitting laser radiation of 213 nm with a pulse width of 4.2 ns and a quadrupole ICP-MS spectrometer Agilent 7500ce (Agilent Technologies, Japan). The ICP-MS parameters were optimized with respect to get the best S/N ratio, RSD, and oxide ratio (ThO^+/Th^+) lower than 0.5% using glass reference material NIST610. The imaging of the dot blots was performed using the following ablation parameters: a laser beam diameter of 110 μm, laser beam fluence of 2.5 J/cm^2, a repetition rate of 10 Hz, a scan speed rate of 150 μm/s, and a distance between individual lines of 115 μm.

The whole spot was ablated line by line and the Au signals of monitored isotopes (^{197}Au, ^{165}Ho) were measured. The limit of quantification for signal intensity is calculated according to tenfold of standard deviation of the gas level (without ablation). All intensities below the limit of quantification were set to zero. The sum of intensities across the whole spot was then calculated. The images of the dot blots were created using lab-made software Laser Ablation Tool for processing of raw data and Excel for presenting the maps as surface plots with the intensity shown in a color-coded intensity scale.

Results and discussion

In biological workflows proteins are usually detected in a Western blot assay after gel electrophoresis and electroblotting onto membranes. Detection is performed by use of tagged antibodies and signals are measured by colloidal gold, fluorescence signals, or by luminescence in the peroxidase and alkaline phosphatase assay, as discussed previously in the "Introduction" section. The whole procedure is prone to protein losses during the separation and electro-transfer process so all quantitative information can be completely lost. However, one of the authors has recently shown that dot blot experiments can overcome this limitation if the specificity of the antibody is high enough to detect the target protein even in complex protein extracts [22].

The workflow of the dot blot analysis and the type of antibody labelling applied in this study is summarized in Fig. 1. In this study, the sensitivity of antibody labelling by a conventionally used MeCAT method using holmium as a lanthanide element with gold nanoparticle-labelled antibodies will be compared. Moreover, two different sizes of nanoparticles (10 nm and 60 nm) will be investigated (Fig. 1a). The overall workflow of the experiment (antibody labelling, dot blot preparation, and LA-ICP-MS analysis) is shown in Fig. 1b.

The number of Au atoms and thus the signal intensity in LA-ICP-MS of AuNPs bound to antibodies is directly proportional to the volume of the NP with a diameter of 10 or 60 nm, if a single particle binding is assumed. The calculated volume of 60 nm NP is 200 times larger than 10 nm NP. Therefore, the signal ratio should be improved by a factor of approximately 200 for the larger particle.

The AuNP-Ab were pipetted in a dilution series of 1:100; 1:1000 and 1:10,000 onto the surface (without antigen) of preconditioned PVDF membrane to evaluate the signal intensity of Au in relation to the nanoparticle size (Fig. 2a). The Au signal of the 60 nm AuNP-Ab conjugate is approximately five times higher (6.7, 4.9, and 5.9 for 100, 1000, and 10,000 times dilution, respectively) compared to the 10-nm AuNP-Ab conjugate diluted to the same absorbance (Table 1). This means that the amount of 10-nm AuNPs is 50 times higher than 60-nm AuNPs, approximately. This can be caused either by the fact that some nanoparticles are not conjugated to the antibody or that one antibody is labelled by 50 nanoparticles, which is highly improbable. Because the precise mechanism of labelling is not known (commercial conjugation), we believe that a combination of both factors is the most probable (bare nanoparticles as well as multiple labelling of one antibody).

Subsequently, the non-specific adsorption, as well as the washing efficiency of the membrane procedure was verified (Fig. 2b). For this purpose, the experiment described in Fig. 2b was performed a second time, but now, extensive washing was applied. Only a few weak signals were observed which demonstrated that washing is efficient to remove adsorbed antibodies labelled by nanoparticles from the membrane. The Au signal decreased to less than 4% of the original value (without washing shown in Fig. 2a). When the 10,000 times diluted NP-Ab conjugates were spotted and washed, the measured intensities were either not distinguishable or slightly above the blank level. The lowest range of intensities in Fig. 2b is 0–700 cps; hence, no signal of Au is visible for these spots. However, the intensities listed in Table 1 are calculated as a sum across the whole dot, from approximately 1500 points (the dimension of the dot is about 50 × 30 ablation points). Hence, the sum of integrated intensities for 10,000 times diluted NP-Ab conjugates reaches about 5000 cps.

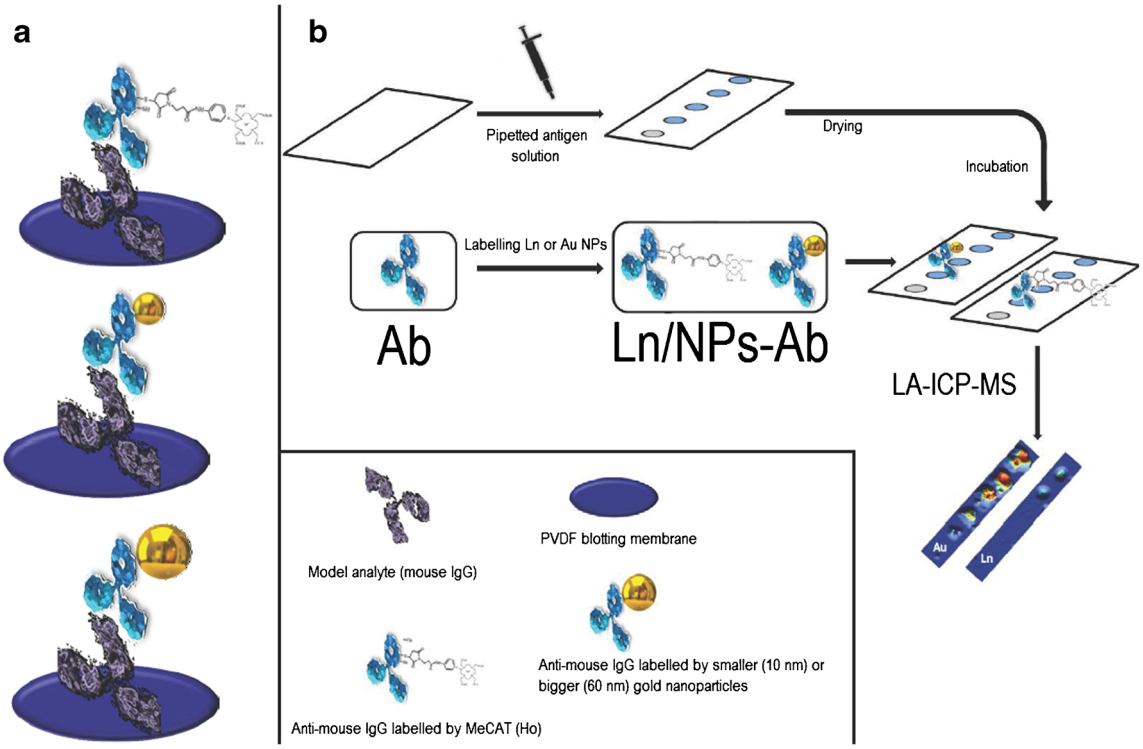

Fig. 1 Workflow of dot blot immunoassay containing the labelled antibodies via non- reduction method (gold nanoparticles) and reduction method MeCAT (Ln). Partially reduced antibodies for MeCAT labelling were obtained by using TCEP solution

Furthermore, the ratio of the Au signal produced by 60 nm NP-Ab and 10 nm NP-Ab conjugates was calculated and its value varied in the range from 4.5 to 8.6 for 100 and 1000 times dilution. These ratios are comparable to the non-washed ratios, which means that the non-specific sorption of the antibody to the PVDF membrane is the same for both types of nanoparticle conjugates and is not dependent on size effects.

Finally, for evaluation of the performance of the labelled antibodies, a titration curve must be measured for a given antigen or AB concentration. For this purpose, we have selected a total antibody amount of 6.66 ng for all antibodies investigated for incubation and changed the total amount of antigen (mouse IgG) in the range from 0.1 to 5 ng. The measured intensities are shown for 60-nm AuNPs (Fig. 3a), 10-nm AuNPs (Fig. 3b), and Ho-MeCAT labelled (Fig. 3c) anti-mouse IgG. Elemental surface plots of the dot blots measured on the membranes are shown together with the integrated intensity of the whole spot area and the calibration graphs. It is clearly seen that the calibration deviates from a linear function in the whole calibration range, and a saturation curve at a higher amount of mouse IgG is observed. This is not surprising because a full saturation of the antigens is expected already in the upper calibration range where the ratio of AB to antigen reaches a 1:1 ratio (the highest amount of antigen and antibody was 5 ng and 6.66 ng, respectively). On one hand, the curvature of the Ab labelled with 60 nm diameter NP looks more pronounced and hints at a steric obstruction of

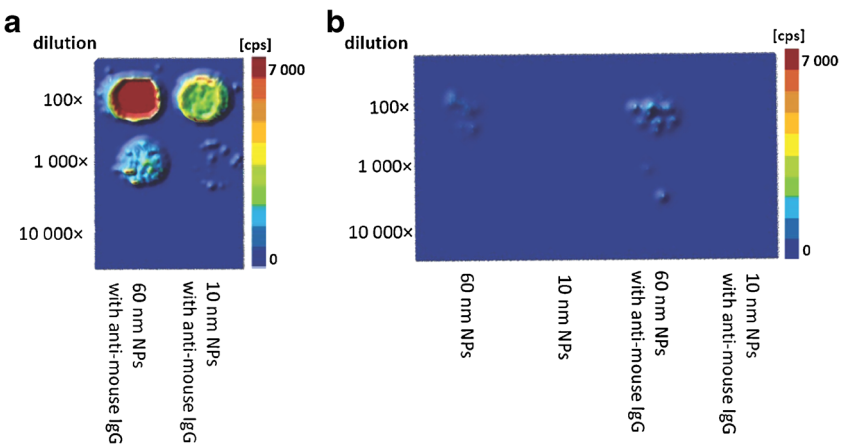

Fig. 2 **a** Elemental maps of Au intensities (cps) of 60-nm and 10-nm AuNPs-Ab conjugates at various dilution in unwashed dot blot. **b** Elemental maps of Au intensities (cps) of 60-nm and 10-nm AuNP-Ab conjugates and 60-nm and 10-nm AuNPs at various dilution in washed dot blot

Table 1 Comparison of the sum of Au intensities for AuNP-Ab conjugates and AuNPs measured in washed and unwashed dot blots. The stock solutions were diluted 100, 1000, and 10,000 times before 0.5 μl was pippeted on the membrane

Dilution	Sum of Au intensities in unwashed dotblot (kcps)		Sum of Au intensities in washed dotblot (kcps)			
	60-nm Au-Ab conjugate	10-nm Au-Ab conjugate	60-nm AuNPs	10-nm AuNPs	60-nm Au-Ab conjugate	10-nm Au-Ab conjugate
100	14,200	2400	340	41	370	82
1000	1200	300	13	7.4	100	12
10,000	97	16	7.4	4.3	7.8	3.3

the large NP, which exceeds the size of a typical antibody of about 15 nm. On the other hand, the smaller molecular weight of MeCAT is the reason for a more linear graph.

For a lower total amount of antigens the calibration graph does show a linear behavior, so the measured intensity can be converted directly to a total amount of antigen applied (if an excess of antibody is used). The slope of the graph can be used for comparison of the three differently labelled antibodies and the following slopes have been calculated: 4.03×10^7, 6.33×10^5, and 2.08×10^3 cps kg mg^{-1} for 60-nm AuNPs, 10-nm AuNPs, and Ho-MeCAT, respectively. It can be concluded from these results that the slopes (sensitivity) of each labelling strategy differs by two orders of magnitude, demonstrating an improvement by four orders of magnitude in the best case. In terms of detection limits (according to 3 σ), absolute values at the picogram levels were calculated in particular 11 pg, 51 pg, and 260 pg for 60-nm AuNPs, 10-nm AuNPs, and Ho-MeCAT, respectively, which again demonstrates that the signal to noise ratio and not the improvement in sensitivity plays the important role in an immunoassay. However, in comparison to MeCAT, a significant improvement in the LOD by at least a factor of 5 (20) can be achieved. The last advantage of Ab labelling by NPs compared to MeCAT is the absence of a reduction step. Before MeCAT labelling it is necessary to partially reduce Ab (reduction of disulphide bridges) and thus some Ab could be reduced so much that it can lead to the loss of its biological function. Labelling by nanoparticles does not require this reduction step, and thereby, NP is conjugated to the whole Ab.

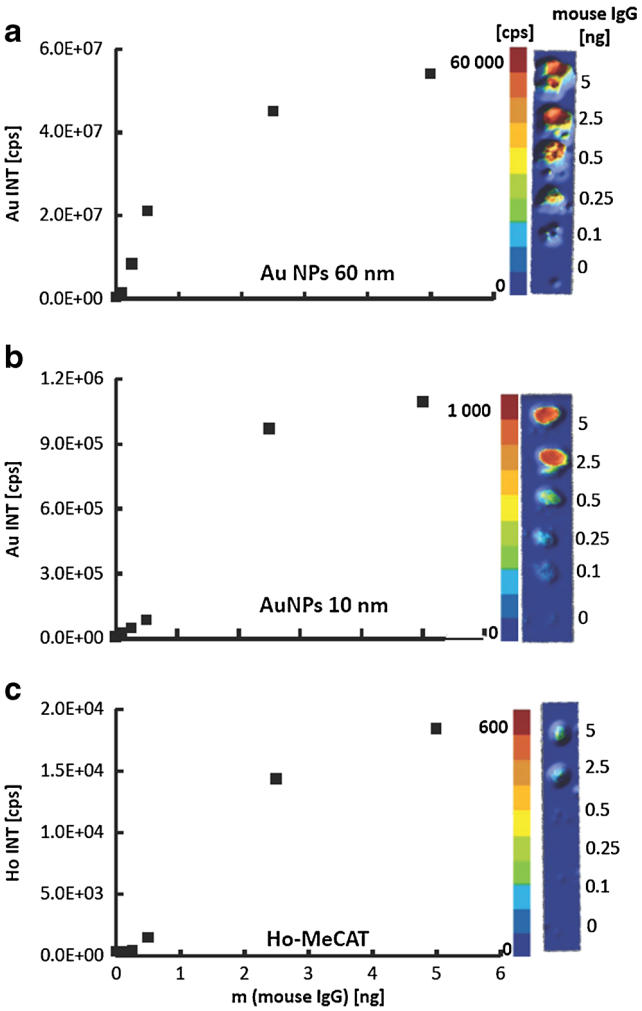

Fig. 3 Au and Ho intensities measured on a PVDF membrane depending on the amount of antigen (mouse IgG).The antibody (anti-mouse IgG) have been labelled by **a** AuNPs—60 nm, **b** AuNPs—10 nm, and **c** Ho-MeCAT; a total amount of 6.66 ng AB has been applied for all three experiments

Conclusion

The labelling strategy of the antibody by nanoparticles with diameters of 10 and 60 nm, respectively, was developed and compared to widely used labelling via MeCAT. The sensitivity of the 60 nm AuNP labelling was improved by 4 orders of magnitude in comparison to MeCAT strategy whereas the LOD is approximately 20 times better. It shows a higher background level for AuNP labelling caused by their non-specific sorption. The forthcoming work is focused on suppression of the non-specific sorption to minimize signal to noise ratio and improve LOD significantly.

Acknowledgments Financial support was provided by Grant Agency of Czech Republic (GACR 17-12774S) and project CEITEC 2020 (LQ1601) with financial support from the Ministry of Education, Youth and Sports of the Czech Republic under the National Sustainability Program II. LPV was supported by project 6SA17676 that received funding from the European Union's Horizon 2020 research and innovation program under the Marie

Skłodowska-Curie and which is co-financed by the South Moravian Region under the grant agreement No. 665860.

Compliance with ethical standards

Conflict of interest The authors declare that they have no conflict of interest.

References

1. Brada D, Roth J. Golden blot - detection of polyclonal and monoclonal-antibodies bound to antigens on nitrocellulose by protein-a gold complexes. Anal Biochem. 1984;142:79–83.
2. Surek B, Latzko E. Visualization of antigenic proteins blotted onto nitrocellulose using the immuno-gold-staining (IGS) method. Biochem Biophys Res Commun. 1984;121:284–9.
3. Hsu YH. Immunogold for detection of antigen on nitrocellulose paper. Anal Biochem. 1984;142:221–5.
4. Dykman L, Khlebtsov N. Gold nanoparticles in biomedical applications: recent advances and perspectives. Chem Soc Rev. 2012;41:2256–82.
5. Omidfar K, Khorsand F, Azizi MD. New analytical applications of gold nanoparticles as label in antibody based sensors. Biosens Bioelectron. 2013;43:336–47.
6. Kang B, Mackey MA, El-Sayed MA. Nuclear targeting of gold nanoparticles in cancer cells induces dna damage, causing cytokinesis arrest and apoptosis. J. Am. Chem. Soc. 2010;132:1517.
7. Kneipp J, Kneipp H, Wittig B, Kneipp K. Following the dynamics of pH in endosomes of live cells with SERS nanosensors. J Phys Chem C. 2010;114:7421–6.
8. Kneipp J, Kneipp H, McLaughlin M, Brown D, Kneipp K. In vivo molecular probing of cellular compartments with gold nanoparticles and nanoaggregates. Nano Lett. 2006;6:2225–31.
9. Drescher D, Zeise I, Traub H, Guttmann P, Seifert S, Buchner T, et al. In situ characterization of SiO2 nanoparticle biointeractions using BrightSilica. Adv Funct Mater. 2014;24:3765–75.
10. Wilschut J, Hoekstra D. Membrane-fusion - from liposomes to biological-membranes. Trends BiochemSci. 1984;9:479–83.
11. Mellman I, Fuchs R, Helenius A. Acidification of the endocytic and exocytic pathways. Annu Rev Biochem. 1986;55:663–700.
12. Kneipp J, Kneipp H, Wittig B, Kneipp K. One- and two-photon excited optical pH probing for cells using surface-enhanced Raman and hyper-Raman nanosensors. Nano Lett. 2007;7:2819–23.
13. Ochsenkuhn MA, Jess PRT, Stoquert H, Dholakia K, Campbell CJ. Nanoshells for surface-enhanced Raman spectroscopy in eukaryotic cells: cellular response and sensor development. ACS Nano. 2009;3:3613–21.
14. Becker JS, Zoriy M, Matusch A, Wu B, Salber D, Palm C. Bioimaging of metals by laser ablation inductively coupled plasma mass spectrometry (LA-ICP-MS). Mass Spectrom Rev. 2010;29:156–75.
15. Buchner T, Drescher D, Merk V, Traub H, Guttmann P, Werner S, et al. Biomolecular environment, quantification, and intracellular interaction of multifunctional magnetic SERS nanoprobes. Analyst. 2016;141:5096–106.
16. Zhang C, Wu FB, Zhang XR. ICP-MS-based competitive immunoassay for the determination of total thyroxin in human serum. J Anal At Spectrom. 2002;17:1304–7.
17. Giesen C, Waentig L, Panne U, Jakubowski N. History of inductively coupled plasma mass spectrometry-based immunoassays. Spectrochim Acta B. 2012;76:27–39.
18. Giesen C, Mairinger T, Khoury L, Waentig L, Jakubowski N, Panne U. Multiplexed immunohistochemical detection of tumor markers in breast Cancer tissue using laser ablation inductively coupled plasma mass spectrometry. Anal Chem. 2011;83:8177–83.
19. Waentig L, Jakubowski N, Hardt S, Scheler C, Roos PH, Linscheid MW. Comparison of different chelates for lanthanide labeling of antibodies and application in a Western blot immunoassay combined with detection by laser ablation (LA-)ICP-MS. J Anal At Spectrom. 2012;27:1311–20.
20. Muller SD, Diaz-Bobe RA, Felix J, Goedecke W. Detection of specific proteins by laser ablation inductively coupled plasma mass spectrometry (LA-ICP-MS) using gold cluster labelled antibodies. J Anal At Spectrom. 2005;20:907–11.
21. M. Cruz-Alonso, B. Fernandez, L. Alvarez, H. Gonzalez-Iglesias, H. Traub, N. Jakubowski, R. Pereiro, Bioimaging of metallothioneins in ocular tissue sections by laser ablation-ICP-MS using bioconjugated gold nanoclusters as specific tags, Microchim. Acta, 185 (2018).
22. Waentig L, Techritz S, Jakubowski N, Roos PH. A multi-parametric microarray for protein profiling: simultaneous analysis of 8 different cytochromes via differentially element tagged antibodies and laser ablation ICP-MS. Analyst. 2013;138:6309–15.